

6-2001

# Separation of chiral controlled substances using capillary electrophoresis

Tania Magoon

*Union College - Schenectady, NY*

Follow this and additional works at: <https://digitalworks.union.edu/theses>

 Part of the [Chemistry Commons](#)

---

## Recommended Citation

Magoon, Tania, "Separation of chiral controlled substances using capillary electrophoresis" (2001). *Honors Theses*. 2077.  
<https://digitalworks.union.edu/theses/2077>

This Open Access is brought to you for free and open access by the Student Work at Union | Digital Works. It has been accepted for inclusion in Honors Theses by an authorized administrator of Union | Digital Works. For more information, please contact [digitalworks@union.edu](mailto:digitalworks@union.edu).

UN  
82  
M211S  
2001

**SEPARATION OF CHIRAL CONTROLLED SUBSTANCES USING  
CAPILLARY ELECTROPHORESIS**

**By**

**Tania Magoon**

\*\*\*\*\*

**Submitted in partial fulfillment  
Of the requirements for  
Honors in the Department of Chemistry**

**UNION COLLEGE  
June, 2001**

## ABSTRACT

MAGOON, TANIA Separation of Chiral Controlled Substances Using Capillary Electrophoresis, Department of Chemistry, June 2001.

The separation of the chiral narcotic propoxyphene by capillary electrophoresis (CE) is the goal of this work. A three-way collaboration between our research group, Professor Isiah Warner (LSU) and the New York State Forensic Investigation Center is underway to separate propoxyphene enantiomers and to develop a protocol for the Forensic Center. We are investigating the application of both polymer surfactants and cyclodextrins as CE additives for the separation of enantiomeric propoxyphene. We have synthesized or obtained several polymerized *N*-undecylenyl-L-amino acid and *N*-undecylenyl-L-dipeptide derivatives as a pseudo-stationary phase in capillary zone electrophoresis for the separation of chiral compounds. Though no separation occurred with the polymers, we do note a definite interaction between the polymers and propoxyphene as evidenced in an increased migration time. We also studied a variety of methylated  $\beta$ -cyclodextrin ( $\beta$ -CD) species, and we have achieved successful separation of propoxyphene with heptakis tri(2, 3, 6-O-methyl)  $\beta$ -CD. We will report the results using these polymers and cyclodextrins.

## ACKNOWLEDGEMENTS

I would like to acknowledge Professor T. C. Werner first and foremost for his outstanding counsel and support for my thesis work. Without his excellent advising, I would not be able to be as independent in my research capabilities as I am now. I am truly grateful.

I would like to also acknowledge my Professor Isiah Warner's group at LSU for their help in the polymer synthesis. I also acknowledge the New York State Forensic Investigation Center for their cooperation in developing this protocol, especially Brian Meinweiser, who helped us tremendously in having this protocol used in their laboratory.

In addition, I would like to acknowledge my fellow chemistry majors who made this year such a wonderful experience. I wish them all the best.

Lastly, I would like to acknowledge my parents, Dr. and Mrs. Inder Magoon for supporting the decisions that I make. I offer great gratitude to my sister, Dr. Anita Magoon, for advising me to attend Union College to study chemistry with such outstanding faculty; without her guidance and support, I would not have achieved all that I have.

## TABLE OF CONTENTS

I.	Abstract	ii
II.	Acknowledgments	iii
III.	Table of Figures	v
IV.	Introduction	1
V.	Experimental	23
VI.	Results	26
VII.	Discussion	56
VIII.	References	63

## TABLE OF FIGURES

Figure 1: Propoxyphene	2
Figure 2: Typical Setup for and Electrophoresis System	5
Figure 3: Electroosmotic Mobility Diagram	7
Figure 4: Flow Profile for Electroosmotic Flow	9
Figure 5: Velocities of Charged and Neutral Species in Capillary Electrophoresis	12
Figure 6: $\alpha$ -, $\beta$ -, and $\gamma$ -Cyclodextrin Structures	14
Figure 7: Interaction of Chiral Compounds, $A_4$ and $A_1$ with Cyclodextrin Molecules	16
Figure 8: Surfactant and Solute Interactions	19
Figure 9: Polymer Surfactants Used in Our Study	21
Figure 10: Resolution vs. Degree of Methylation	29
Figure 11: Peak Area vs. [Propoxyphene]	33
Figure 12: Order of Elution	36
Figure 13: Variation in Migration Time and Resolution as a Function of pH	40
Figure 14: Electropherogram Comparing Results with Varying Concentrations of Buffer	43
Figure 15: Resolution vs. [CAPS]	45
Figure 16: Optimal Conditions for Separating Propoxyphene	47
Figure 17: Electropherogram Depicting Results with Various Polymer Surfactants	50

Figure 18: Electropherogram Depicting Results with  
poly-L-SUTBL

52

## Introduction

The goal of this work is to develop a simple and efficient protocol for the separation of the enantiomers of the chiral drug propoxyphene (Figure 1) using capillary electrophoresis (CE). One enantiomer of propoxyphene is controlled whereas the other is not. We are collaborating with the New York State Forensic Investigation Center to develop this protocol.

Propoxyphene is an analgesic that is also listed as a Schedule IV controlled substance by the Drug Enforcement Agency (DEA).<sup>1</sup> Patented by Lilly in 1955 and approved by the FDA in 1957, propoxyphene (commercially known as Darvon) is prescribed for the relief of moderate pain; individuals who have undergone surgery or major injuries take propoxyphene. This drug has an interesting biological activity in the brain. Essentially, it decreases not only the feeling of pain in the brain, but it also reduces the emotional response to pain. The major drawback to this drug, however, is that it becomes habit-forming. There are many side effects to this drug including depression, hallucinations, lightheadedness, and blurry vision. Symptoms of drug overdose include coma, convulsions, irregular heartbeat, and stupor.<sup>2</sup> Thus the habit-forming nature of the drug combined with its euphoric side effects contributes to its severe abuse in the United States. In fact, it is one of the most abused drugs in the United States.

Propoxyphene has two stereoisomers with analgesic activity, the  $\alpha$ -dl- and d-diastereoisomers. In contrast, the  $\beta$ -diastereomer is quite inactive, and it is not used as an



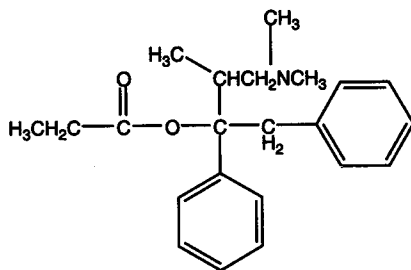


Figure 1. Propoxyphene

analgesic.<sup>3</sup> Propoxyphene is commercially sold in two forms—as the hydrochloride salt and also the napsylate salt. Propoxyphene napsylate differs from propoxyphene hydrochloride in that it allows more stable liquid dosage forms and tablet formulations.<sup>4</sup>

The current method of separation that is used by the Forensic Center takes advantage of one of the properties of chiral substances; namely that a certain enantiomer, say d, will only crystallize with other d enantiomers of the same compound. Crystallization will not occur if both d and l are present. The Forensic Center therefore takes the sample that is under suspect, dissolves it with a standard of the l form, and attempts to grow crystals. If crystals are formed, then the sample was in the l form; on the other hand if crystals do not appear, the sample was in the d form. Although one might consider this to be an acceptable method of analysis, serious problems do exist. One problem is that determining the presence of crystals is a relatively difficult and tedious process. In addition, there is no hard copy of the data to which an investigator can refer in a court case; issues of reasonable doubt then surface. Moreover, a relatively large sample (greater than a milligram) is needed for the analysis. These issues demand a more efficient method of analysis that produces a hard copy of the data and allows the detection of a small amount of sample.

One powerful method of separation that is gaining popularity is capillary electrophoresis (CE). In contrast to other, more conventional systems such as gas chromatography (GC) or high performance liquid chromatography (HPLC), CE has the advantage of having higher separation efficiency and resolution, faster analysis times,

and smaller sample volumes.<sup>5</sup> One of the major advantages of CE, over direct chiral HPLC separation, is that only a few millilitres of buffer are needed for separation in CE.<sup>5</sup>

Electrophoresis involves the separation of species in solution based on their charge-to-mass ratio. Although four modes of separation do exist, including moving-boundary electrophoresis (MBE), zone electrophoresis (ZE), isotachopheresis (ITP) and isoelectric focusing (IEF), only zone electrophoresis will be discussed since this is the separation mode that we used. In ZE, species are introduced into a buffer-filled capillary that is made of fused silica with a typical internal diameter of 50  $\mu\text{m}$ . The buffer reservoirs, which are placed at both ends of the capillary, contain electrodes across which a potential (~20-30 kV) is applied. Normally, the negative electrode is placed at the end of the capillary where the detector is located (See Figure 2).<sup>6</sup>

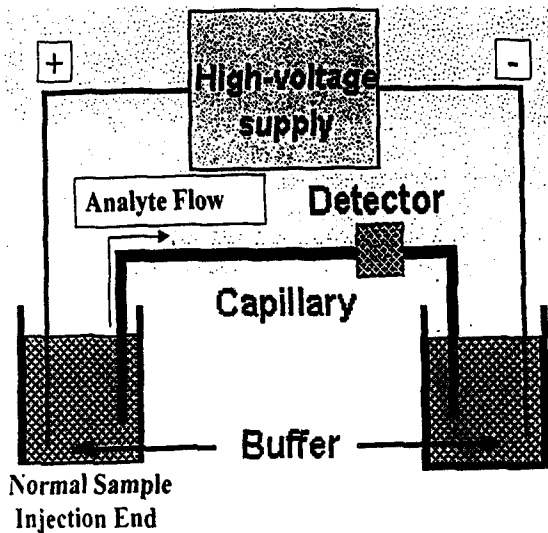


Figure 2. Typical setup for an electrophoresis system. (Reproduced from [www.scimedia.com/chem-ed/sep/electrop/cap-el.htm](http://www.scimedia.com/chem-ed/sep/electrop/cap-el.htm))

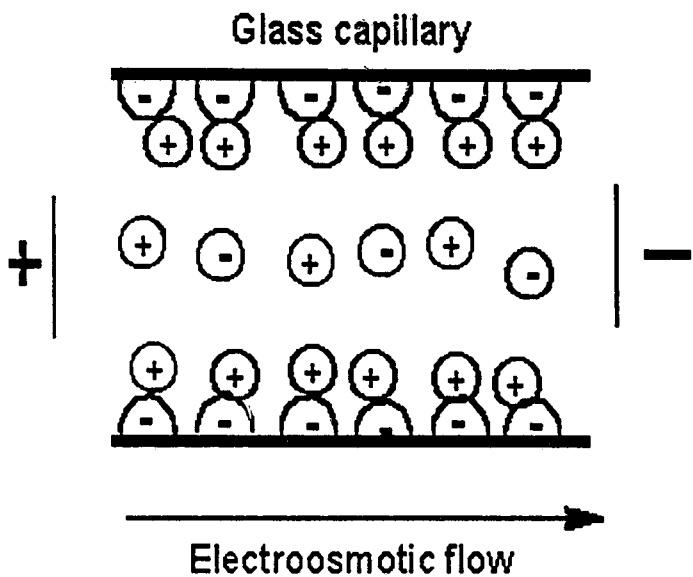
This applied voltage then creates an electric field that separates analytes based on their charge-to-mass ratio. Two driving forces are at work in separating species in  $\perp E$ : electrophoretic mobility and electroosmotic mobility.

The electrophoretic mobility (EPM or  $\mu_{ep}$ ) is obtained by utilizing electrical forces along the axis of an electrical field gradient. The electrophoretic mobility of an analyte is directly proportional to its charge and inversely proportional to frictional forces that are determined by the radius and shape of the analyte and viscosity of the buffer.<sup>7</sup>

$$\mu_{ep} = \frac{Q_{eff}}{6\pi\eta R} \quad (1)$$

In this equation  $\mu_{ep}$  is the effective electrophoretic mobility ( $\text{cm}^2 \text{s}^{-1} \text{V}^{-1}$ ),  $Q_{eff}$  is the effective charge (C) of the ion,  $\eta$  is the Newtonian viscosity (Pa s) of the solution, and  $R$  is the total radius (cm) of the ion. From this equation it can be deduced that neutral species have a zero electrophoretic mobility while cations have a positive  $\mu_{ep}$  and anions have a negative  $\mu_{ep}$ . If electrophoretic mobility were the only driving force in the system then only the positively charged species would reach the detector. However, this is not the case since another driving force, the electroosmotic mobility, is also at work.

The phenomenon known as electroosmotic mobility (or flow) results from the relative motion of a liquid to a fixed charged surface caused by an electric field.<sup>7</sup> Electroosmotic mobility is produced by an electric double layer formed between the capillary wall and buffer. The silanol groups of the capillary are ionized to create a negative charge on the wall, and buffer cations are attracted to the negatively charged capillary surface to form a charged double layer. Cations that are close to this double



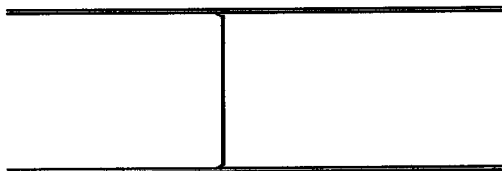
©1995 CHP

Figure 3. Electroosmotic Mobility Diagram. (Reproduced from [www.scimedia.com/chem-ed/sep/electrop/cap-el.htm](http://www.scimedia.com/chem-ed/sep/electrop/cap-el.htm))

layer are also at the same time pulled towards the negative electrode at the capillary end; these buffer cations pull the rest of the solution and the analytes through the capillary (Figure 3).<sup>6</sup>

This generates a flat flow profile in the capillary, in contrast with the laminar, or parabolic, flow profile generated by pressure-driven systems such as LC or GC (Figure 4).<sup>8</sup> This type of flow causes the analytes to elute in a thin, flat profile rather than as a spread of material, causing the sharp peaks often seen in CE electropherograms.

**Cross-Sectional Flow Profile  
Due to Electroosmotic Flow**



**Cross-Sectional Flow Profile  
Due to Hydrodynamic Flow**

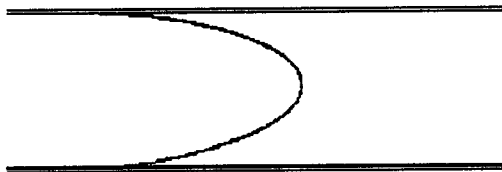


Figure 4. The plug profile for the electroosmotic flow (above) is contrasted with the parabolic, or laminar, flow that is caused by hydrodynamic flow. (Reproduced from [www.ceandcec.com/cetheory.htm](http://www.ceandcec.com/cetheory.htm))



One can calculate the electroosmotic mobility by using the following equation:

$$\mu_{eo} = \frac{\zeta \epsilon}{4\pi\eta} \quad (2)$$

Where  $\zeta$  is the zeta potential (the voltage across the diffuse double layer),  $\epsilon$  is the permittivity of the solution, and  $\eta$  is the viscosity of the buffer.<sup>7</sup>

One important factor to keep in mind in electrophoresis is the pH range within which a system can operate. If the pH is too low (below 2.5), then all of the silanol groups are protonated, and there is no attraction between the buffer cations and the capillary wall. This eliminates the electroosmotic mobility. On the other hand, pH values larger than 8 do not significantly increase the magnitude of the flow since mostly all of the silanol groups are deprotonated.<sup>7</sup>

Both these concepts of electroosmotic and electrophoretic flow can be combined to give an analyte's total, or apparent mobility,  $\mu_{app}$ :

$$\mu_{app} = \mu_{eo} + \mu_{ep} \quad (3)$$

For neutral species  $\mu_{app}$  is equal to  $\mu_{eo}$  since  $\mu_{ep}$  is zero. For positive species  $\mu_{app}$  is greater than  $\mu_{eo}$  since  $\mu_{ep}$  is positive, and  $\mu_{app}$  for negative species is less than  $\mu_{eo}$  since  $\mu_{ep}$  is negative. The mobilities of various species can be represented as vectors (Figure 5).

The apparent mobility of an analyte can also be determined from its net velocity,  $v_{net}$  divided by the applied electric field (E):

$$\mu_{app} = v_{net}/E = (L_d/t)/(V/L_t) \quad (4)$$

In this equation  $L_d$  is the length of the capillary from injection to the detector,  $t$  is the migration time,  $V$  is the applied voltage between the two electrodes, and  $L_t$  is the total

length of the capillary. The value of  $\mu_{app}$  is essentially the proportionality constant between the velocity of an analyte and the electric field.

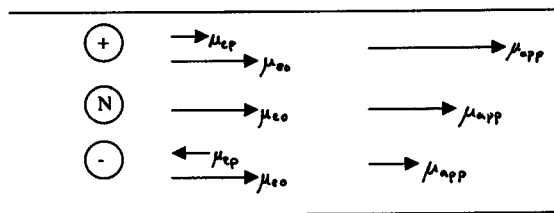


Figure 5. Velocities of charged and neutral species in capillary electrophoresis

We have seen how CE can be used to separate species based on their charge-to-mass ratio. However, if different species have the same charge-to-mass ratio, such as enantiomers, we must be subtler in our method of separation. Chiral separation in CE is performed in a variety of ways, one of which is the addition of chiral selectors into the mobile phase. Such selectors include cyclodextrins, chiral metal complexes, and chiral surfactants.<sup>9</sup> Separation using micelles is commonly known as micellar electrokinetic capillary chromatography (MECC or MEKC).

Cyclodextrins (CDs) have been used extensively in the separation of a variety of compounds.<sup>10</sup> CDs are made of 6, 7, or 8 glucopyranose rings and are called  $\alpha$ -,  $\beta$ -, and  $\gamma$ -CD, respectively. They have a torroidal shape, and the hydrophobic inner cavity have different sizes, depending on the type of cyclodextrin. It is believed that chiral separation results from both hydrogen bonding between the molecule and the larger hydroxy rim and interactions between the molecule and the chiral hydrophobic interior of the CD.<sup>11</sup> CDs are inexpensive, easy to use, and readily available. Moreover, many different types of CDs exist; there are not only different sizes, but they also contain certain functionalities that can be employed to afford better separation.<sup>10</sup> These functional groups can render the CD either neutral or charged, further expanding the variety of CDs. Figure 6 shows typical cyclodextrins.<sup>11</sup>

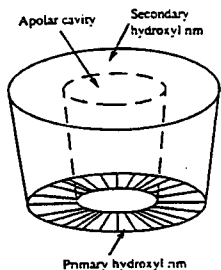
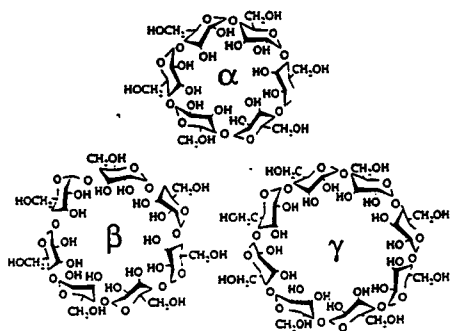


Figure 6.  $\alpha$ -,  $\beta$ -, and  $\gamma$ -CD structures. (Reproduced from I. S. Lurie, *Analysis of Seized Drugs by Capillary Electrophoresis*)

$\alpha$ -CD has a cavity of 4.7-6 Å (its form is akin to a rectangular torroid) while  $\beta$ -CD has a cavity size of 8 Å.  $\gamma$ -CD has the largest cavity of the three—10 Å.<sup>10</sup> One rule of thumb is that the  $\alpha$ -CD allows a molecule the size of a phenyl ring or smaller to enter. This inner cavity can allow species to partition in and out, depending on the size of the species and magnitude of molecular contact. When a species interact with the cyclodextrin its charge-to-mass ratio is affected, and its overall mobility changes. Thus, one enantiomer may have more preference to interact with the cyclodextrin over the other enantiomer, and, as a result, the mobility of this enantiomer will become different from that of the other enantiomer. This change in the mobilities results in the separation of the enantiomers (Figure 7).<sup>12</sup>

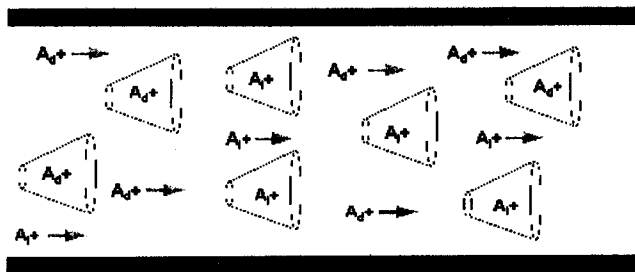


Figure 7. Interaction of chiral compound,  $A_d$  and  $A_p$ , with cyclodextrin molecules.  
 (Reproduced from [www.ceandcec.com/newpage12.htm](http://www.ceandcec.com/newpage12.htm))

The cyclodextrins that we used have a varying degree of methylation; methylation tends to increase the solubility of a CD. Note the 2,3, and 6 hydroxyl positions of one glucopyranose unit in the cyclodextrin. These positions can be methylated to afford different types of cyclodextrins. A cyclodextrin that is dimethylated is usually methylated at the 2 and 6 positions, while a trimethylated CD has methyl groups on all three positions. These methyl groups can make subtle changes in the shape of the cyclodextrin and can modify the interactions between the cavity and guest molecule in a way that affords better (or worse) separation. We decided to use these methylated cyclodextrins to effect the separation of the enantiomers of propoxyphene. The parent cyclodextrin that is most useful with respect to its cavity size is the  $\beta$ -CD; we therefore studied various forms of methylated  $\beta$ -CDs. It should be noted here the propoxyphene has been separated by the use of CDs.<sup>13</sup> Lurie and co-workers were able to separate propoxyphene using a mixture of sulfated  $\beta$ -CD and a dimethylated  $\beta$ -CD in a buffer that contained an organic solvent. Moreover, the analysis took twenty minutes.

Cyclodextrins can also be polymerized by reaction of a CD monomer with polychlorohydrin. The CDs in cyclodextrin polymers (CDPs) are linked by a glyceryl linkers  $[-(\text{CH}_2\text{-CHOH-CH}_2\text{-})_n]$ . These polydisperse mixtures contain 1-5 CDs and have a molecular weight of 11,000. We also used these polymers in our attempt to separate propoxyphene.

Another chiral selector that has been used for the separation of chiral substances is chiral micelles. This method involves the addition of chiral surfactants to the eluent buffer at a concentration that would lead to the formation of micelles. This concentration



is known as the critical micelle concentration (CMC). The relatively high CMC that is needed to form micelles along with the dynamic equilibrium that exists between the micelle and the surfactant molecules (Figure 8a) presents problems that render this an inefficient method. (The "S" denotes solute and the "\*" denotes the chiral center on the surfactant.)<sup>9</sup>

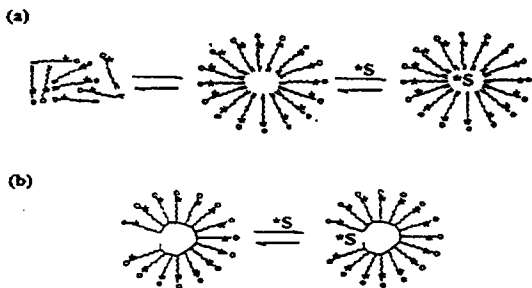


Figure 8. Surfactant and Solute Interactions in traditional (a) and polymerized surfactant micelles. (Reproduced from Wang, J., Warner, I. M. *Anal. Chem.* 1994, 66 (21), 3773-3776.)

To correct for these issues, systems involving polymerized micelles have been introduced. Polymerized micellar systems have significant advantages over traditional micelles. First, they eliminate the aforementioned dynamic equilibrium, since the monomer surfactant molecules are polymerized by covalent bonds (Figure 8b). A second advantage is that polymer surfactant systems enhance the mass transfer rate between the analyte molecule and the micelle itself. In traditional micelles, the analyte molecule transfers deep into the interior of the micelle; in polymerized surfactants the analyte molecule does not transfer as deep into the activity, and this increases the mass transfer rate, resulting in sharper peaks. Finally, the fact that these monomer surfactant molecules are already polymerized into a micelle eliminates the CMC. This is advantageous since high concentrations of surfactant generate heat, causing non-ideal deviations in CE operation.<sup>9</sup>

Warner and co-workers have been able to separate chiral compounds with hydrogen-bond donating capabilities using these polymer surfactants.<sup>5, 9, 14, 15, 16, 17</sup> Figure 9 outlines the polymers that our group has studied.

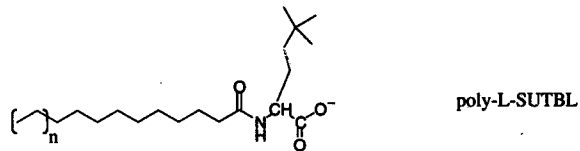
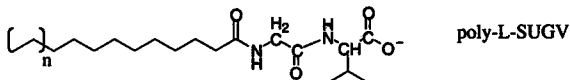
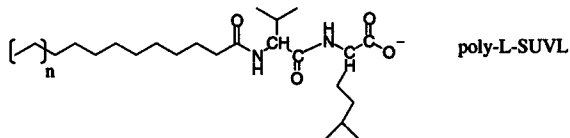
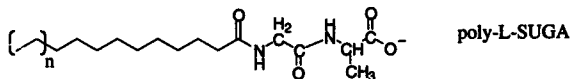
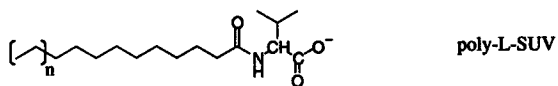


Figure 9. Polymers used in our study. Poly-L-SUG is poly-L-sodium undecylenyl glycine. G represents glycine, A is alanine, V is valine, L represents leucine, and TBL is *tert*-butyl leucine.

Since propoxyphene has a hydrogen-bond accepting group we decided to synthesize a surfactant using threonine as the chiral group on the surfactant. We hope to utilize this hydrogen-bond capability in our efforts to separate the enantiomers of propoxyphene.

## Experimental.

**Chemicals and Reagents.** The napsylate salts of dextro and levo propoxyphene were purchased from the USP Chemical Company. The dextropropoxyphene hydrochloride and CAPS (3-cyclohexylamino-1-propanesulfonic acid) were purchased from Sigma. The boric acid, monobasic dihydrogen phosphate, heptakis di(2,6-O-methyl)  $\beta$ -CD, and heptakis tri(2,3,6-O-methyl)  $\beta$ -CD were purchased from Aldrich Chemical Company. The dimethylated  $\beta$ -CD was a gift from Cerestar. The pH of the buffers was adjusted using appropriate grade 1 M HCl and 1 M NaOH.

The polymers poly-L-SUV and poly-L-SUTBL were synthesized by Nerozzi and Jakubowski. Poly-L-SUVL, poly-L-SUGA, and poly-L-SUGV were synthesized and provided by Dr. Warner's group at LSU. Poly-L-SUThr was synthesized by our group.

**CE.** All experiments were performed on a Hewlett Packard (HP) 3D CE instrument. The following outlines the parameters that were used for sample analysis.

Pressure Injection	50 mbar for 4 seconds
Capillary Length and ID	64.5 cm and 50 $\mu$ m ID
Capillary Temperature	25° C
Detection Wavelength	210 and 220 nm
Voltage	20 kV

For each run, the capillary was flushed for five minutes with the sample buffer prior to injection.

**Polymer Work.** We synthesized the threonine derivative according to the procedure outlined by Mocossay, Shamsi, and Warner with some alterations.<sup>18</sup>

**Undecylenic acid ester.** One-hundred and twenty-five mmol of *N*-hydroxysuccinimide (NHS) was dissolved in 300 mL of ethyl acetate (dried over molecular sieves for 24 hours) and was added to a round-bottom flask. One equivalent (125 mmol) of undecylenic acid was dissolved in 242 mL of dry ethyl acetate, and this solution was added to the flask. Solution was mixed via mechanical stirring. A 1M solution of dicyclohexylcarbodiimide (DCC) (125 mmol) in dry ethyl acetate was added to the round-bottom flask, causing the solution to become cloudy. The reaction was allowed to proceed for 16 hours. The white precipitate dicyclohexylurea (DCU) was removed through vacuum filtration, and the solvent was removed via rotary evaporation, leaving an oil that subsequently crystallized into a waxy product. The product was recrystallized in 100 mL isopropyl alcohol and dried under a high vacuum with a percent yield of 64.7%.

**Threonine Derivative of Undecylenic Acid.** Twenty mmol of the undecylenic acid ester was dissolved in 100 mL THF and poured into a round-bottom flask containing 20 mmol L-threonine and 20 mmol  $\text{Na}_2\text{CO}_3$  in 200 mL deionized water. The solution was allowed to react for 16 hours under mechanical stirring. The pH of the resulting solution was dropped to 2 using 1M HCl. The solvents were removed through rotary evaporation.

Eighty mL of  $\text{CH}_2\text{Cl}_2$  was added to suspend the white product. The product was isolated using gravity filtration with a 42% yield.

**Conversion of the Threonine Derivative of Undecylenic Acid to the Corresponding Salt.** A 1M solution of  $\text{NaHCO}_3$  (8.4 mmol) in water was added to a round-bottom flask containing a 1M solution of the threonine derivative (8.4 mmol) in THF. The solution was allowed to react for 24 hours. The solvent was removed by evaporation. The monomer was polymerized by  $\text{Co-}\gamma$  radiation source at Louisiana State University.

We are also synthesizing peptide derivatives of threonine using hexanoic acid and 4-pentenoic acid. We used the procedure outlined above.



## Results.

### *Monomer Cyclodextrin Study*

We first tried a variety of derivatized CDs, examining the changes in migration times and resolution in the propoxyphene peak. We used a 25 mM borate buffer with 300 mM CAPS in all cases. Table 1 lists the different types of cyclodextrins used along their concentrations.

The first dimethylated  $\beta$  CD (DM- $\beta$ -CD) was a gift from Cerestar; it is listed as being slightly overmethylated, which means that it actually has slightly more than the predicted fourteen methyl groups in a dimethylated  $\beta$ -CD.<sup>19</sup> A resolution of approximately 1.0 is achieved at a pH of 9.23, whilst at a higher pH of 9.68, the resolution decreases to about 0.88 (Table 1).

Next we tested another dimethylated  $\beta$ -CD (DM- $\beta$ -CD) purchased from Aldrich. The literature accompanying this CD stated that this product is slightly undermethylated; it has less than fourteen methyl groups. At 10 mM of the CD we see a resolution of 0.75, and at 20 mM of the CD we see a resolution of 0.81. Thus, a reduced methylation appears to reduce the resolution (Table 1).

With this information we decided to test a heavily methylated  $\beta$ -CD, believing that an increase in the number of methyl groups will increase the resolution of the two peaks. We examined heptakis tri(2,3,6-O-methyl)  $\beta$ -CD (TM- $\beta$ -CD) at a pH of 9.66, and the resolution increased from 1.02 to 1.76 to 1.86 with increasing concentrations of CD (10 mM to 20 mM to 30 mM) (Table 1).

We then tried a hydroxypropyl  $\beta$ -CD at a pH of 9.66, and no separation occurred.

**Table 1. Resolution and Migration Time for Propoxyphene Using Various Types of Cyclodextrins**

10 mM DM $\beta$ -CD (Cerestar)	9.23	0.025	4.55	1.02
20 mM DM $\beta$ -CD (Cerestar)	9.23	0.025	4.93	1.03
30 mM DM $\beta$ -CD (Cerestar)	9.23	0.025	5.14	0.98
10 mM DM $\beta$ -CD (Cerestar)	9.23	0.025	9.54	0.98
20 mM DM $\beta$ -CD (Cerestar)	9.23	0.025	10.49	0.93
10 mM DM $\beta$ -CD (Cerestar)	9.68	0.025	5.14	0.88
20 mM DM $\beta$ -CD (Cerestar)	9.68	0.025	5.37	0.87
10 mM DM $\beta$ -CD (Cerestar) and 10 mM Alpha CD	9.66	0.025	4.94	0.81
10 mM DM $\beta$ -CD (Aldrich)	9.66	0.025	4.67	0.75
20 mM DM $\beta$ -CD (Aldrich)	9.66	0.025	5.06	0.81
10 mM TM $\beta$ -CD (Aldrich)	9.66	0.025	4.66	1.02
20 mM TM $\beta$ -CD (Aldrich)	9.66	0.025	4.91	1.76
30 mM TM $\beta$ -CD (Aldrich)	9.66	0.025	5.18	1.86
10 mM Hydroxy Propyl	9.66	0.025	4.5	0
20 mM Hydroxy Propyl	9.66	0.025	4.8	0

We believe that the longer chains might be altering the binding cavity (Table 1).

We finally tried a combination of Cerestar DM- $\beta$ -CD (10 mM) and an  $\alpha$ -CD (10 mM). Separation did indeed occur, since the resolution was calculated to be 0.81. However, since this system is more complicated (two CDs instead of one), and also since better resolutions were achieved with the other methylated  $\beta$ -CDs, we decided not to pursue this system (Table 1). Figure 10 shows the general trend of increasing resolution with increasing degree of methylation. The concentration of CD for each type is 20 mM.

Table 2 shows a summary of the data concerning the use of different types of methylated  $\beta$ -CDs. In each run, the sample concentration was 0.025 mg/mL l- and 0.025 mg/mL d- propoxyphene. For each CD, the resolution increases with increasing CD concentration. The last two entries in Table 5 indicate variations that we performed on the method for the trimethylated cyclodextrin. In the first of the two we increased the concentration of the borate buffer from 25 to 75 mM. We see an increase in the resolution, but we also see an increase in the migration time of the peak (6.87 minutes compared to 5.18 minutes). In the last of the two entries we lowered the pH to 8.23, keeping the borate buffer concentration at 25 mM, and noted a significant improvement in the shape of the peaks and resolution. The resolution increased to 3.32, and the migration time increased to 6.08 minutes. As a consequence, we consider these conditions to be optimal for propoxyphene separation.

Figure 10. Resolution vs. Degree of Methylation

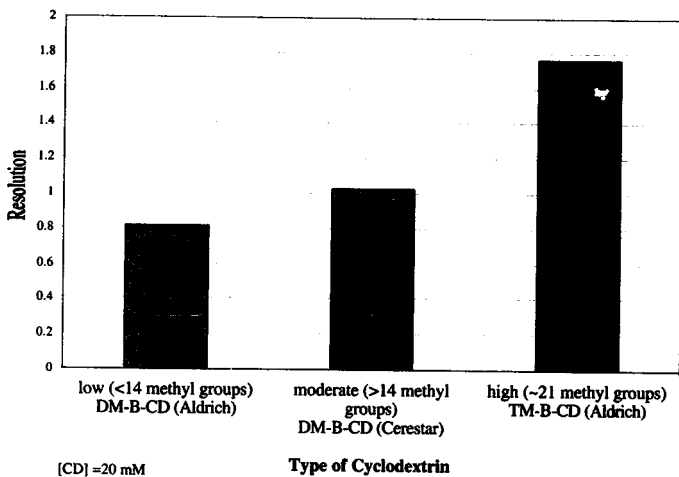


**Table 2. Comparison of Migration Times and Resolutions for Differing Cyclodextrins**

Table 2. Comparison of Migration Times and Resolutions for Differing Cyclodextrins					
		$t_m$			
DM- $\beta$ -CD (Aldrich)	10	9.66	25 mM	4.67	0.75
DM- $\beta$ -CD (Aldrich)	20	9.66	25 mM	5.06	0.81
DM- $\beta$ -CD (Cerestar)	10	9.68	25 mM	5.14	0.88
DM- $\beta$ -CD (Cerestar)	20	9.68	25 mM	5.37	0.87
TM- $\beta$ -CD (Aldrich)	10	9.66	25 mM	4.66	1.02
TM- $\beta$ -CD (Aldrich)	20	9.66	25 mM	4.91	1.76
TM- $\beta$ -CD (Aldrich)	30	9.66	25 mM	5.18	1.86
TM- $\beta$ -CD (Aldrich)	30	9.66	75 mM	6.87	2.00
TM- $\beta$ -CD (Aldrich)	30	8.23	25 mM	6.08	3.32

Increasing  
Degree  
of  
Methylation



<sup>1</sup> 300 mM CAPS (4-[Cyclohexylamino]-1-butanesulfonic acid)

<sup>2</sup>  $t_m$  is average of both L and D peaks

Since we found an optimal method of separation we wanted to explore its quantitative aspects. We decided to first see how reproducible the peak areas were for the runs with respect to one another. A run of 0.025 mg/mL 1- and 0.025 mg/mL d-propoxyphene with 25 mM borate buffer, 300 mM CAPS, and 30 mM heptakis tri(2,3,6-O-methyl)  $\beta$ -CD at pH 8.23 was performed in triplicate. Table 3 shows the results from these runs.

**Table 3. Reproducibility of Peak Area**

2.34	2.53	4.14	4.55	9.43	10.5
2.26	2.55	4.12	4.49	9.9	10.9
2.30	2.54	4.21	4.48	9.67	10.7
2.30	2.54	4.16	4.51	9.67	10.70
0.04	0.01	0.05	0.04	0.2	0.2
<b>1.7</b>	<b>0.4</b>	<b>1.1</b>	<b>0.8</b>	<b>2.4</b>	<b>1.9</b>

The relative standard deviation for the peak areas agrees well with the reported relative standard deviation of 1% (Agilent Technologies). One reason for the slight fluctuation in values may be inconsistencies in the placement of the baseline when calculating the peak areas. Such fluctuation would cause mild variations in the integration.

The average areas of the peaks were plotted against the concentration of the samples (Table 4 and Figure 11).

**Table 4. Average Peak Area for Different  
[Propoxyphene]**

0.0125	2.42
0.025	4.33
0.050	10.2

The high linearity indicates that this method could be used for quantitative analysis. We also performed an analysis on a propoxyphene sample at a concentration of 0.075 mg/mL (of both enantiomers). We attempted to incorporate these data with the previous data to determine the full range of concentrations at which we could quantify an unknown sample of propoxyphene. This resulted in a very poor standard curve. We therefore determined that our method could quantify propoxyphene from 0.0125 to 0.05 mg/mL.

**Figure 11. Peak Area vs.  
[Propoxyphene]**

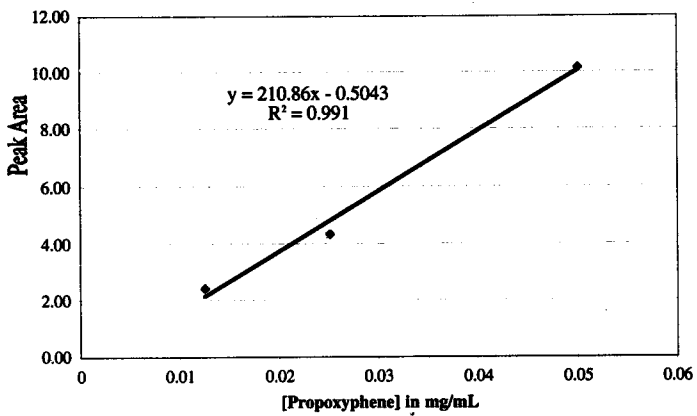




Table 5 shows migration times and peak area data from a triplicate run of 0.025 mg/mL of l and d propoxyphene enantiomers with 30 mM trimethylated  $\beta$ -CD. The average relative standard deviation for the migration times is 0.2% whereas the relative standard deviation for the peak areas is 1%.

**Table 5. Reproducibility of Data with 30 mM of TriMethylated Beta CD and 0.025 mg/mL Propoxyphene**

1	5.17	5.22	4.14	4.55	1.53
2	5.15	5.21	4.12	4.49	1.58
3	5.14	5.20	4.21	4.48	1.63
AVERAGE	5.15	5.21	4.16	4.51	1.58
STDEV	0.01	0.01	0.04	0.04	0.05
REL STDEV (%)	0.2	0.2	1	0.9	3

Tables 6a and 6b show data from experiments in which we added methanol and acetonitrile to a 25 mM borate buffer containing 20 mM Cerestar dimethylated  $\beta$ -CD and 300 mM CAPS at a pH of 9.61. These substances, which were added at 1, 3, and 5 (v/v)%, can modify the cavity of the cyclodextrin and thereby improve separation. The first additive was methanol, and we used methanol in 1%, 3%, and 5% (v/v%) solutions.

We did not observe any significant change in the resolution, nor could we determine any trend in increasing the concentration of methanol or acetonitrile.

**Table 6a. Effect of MeOH on 20 mM of Cerestar Dimethylated Beta CD**

1	5.500	5.528	0.93
3	5.972	6.005	1.02
5	6.301	6.336	0.99

**Table 6b. Effect of AcCN on 20 mM of Cerestar Dimethylated Beta CD**

1	5.426	5.454	0.93
3	5.762	5.793	1.00
5	5.839	5.869	0.94

To determine the order of elution of the l and d enantiomers, we made a 2:1 solution (0.050 mg/mL : 0.025 mg/mL) of l to d propoxyphene. We ran this sample with a 25 mM borate buffer with 30 mM Heptakis tri(2,3,6-O-Methyl)  $\beta$ -CD and 300 mM CAPS. Our results indicate that the l form elutes first (Figure 12).

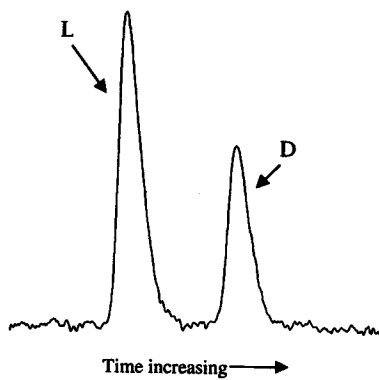


Figure 12. Order of Elution

*Polymer CDs*

We also tried a variety of cyclodextrin polymers (CDPs), specifically  $\alpha$ -,  $\beta$ -, and  $\gamma$ -CDP (Table 7). From our data we concluded that 30 mM  $\gamma$ -CDP resulted in the best resolution (4.45). The MTs for the peaks for this run were 6.688 and 6.953 minutes. Although this is a longer analysis time, it still is relatively fast. (*For more information on the results from the CDP study please refer to Keiko Ota's thesis.*)

**Table 7. Polymer Cyclodextrin (CDP) Data pH 8.25**

$\beta$ CDP	10 mM	4.689	4.722	0.100	0.7	5.6	3.23E-06
	20 mM	5.270	5.313	0.070	1.2	6.2	2.91E-06
	30 mM	6.102	6.164	0.114	1.1	7.1	2.54E-06
$\gamma$ CDP	5.7 mM	4.504	4.524	0.050	0.8	5.4	3.34E-06
	11.4 mM	4.817	4.849	0.054	1.2	5.6	3.23E-06
	17.1 mM	5.011	5.048	0.062	1.2	5.8	3.11E-06
	10 mM	5.804	5.846	0.089	0.9	7.1	2.54E-06
	20 mM	6.262	6.319	0.099	1.2	7.4	2.43E-06
	30 mM	6.688	6.953	0.119	4.5	8.0	2.26E-06
$\alpha$ CDP	no separation						

### Method Optimization

From the earlier studies on monomer cyclodextrins, we decided to optimize the experimental conditions using the heptakis tri(2,3,6-O-methyl)  $\beta$ -CD purchased from Aldrich. The method was optimized with respect to the parameters of pH, borate buffer concentration, and concentration of CAPS. The following outlines the results from these studies.

### *Buffer pH Optimization*

We tested a range of buffer pH values to determine the effect of pH on resolution, electroosmotic flow, and electrophoretic flow. Table 14 lists the migration times and resolution values for a range of pH values about the  $pK_a$  of the buffer. (The  $pK_a$  of boric acid is 9.2).

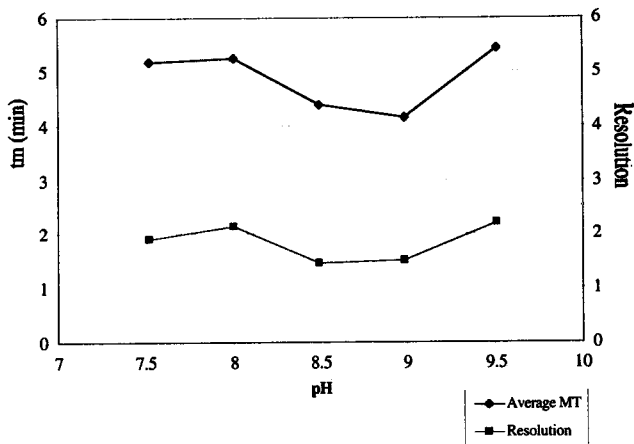
**Table 8. Migration Times and Resolution at Different pH Values**

7.52	5.148	5.23	6.548	1.91
8.00	5.209	5.292	6.576	2.16
8.49	4.359	4.412	5.162	1.47
8.98	4.132	4.181	4.764	1.51
9.51	5.413	5.484	6.188	2.22

(Note that the methanol peak is used as a EOF marker; its migration time marks the electroosmotic flow.)

Figure 13 shows the average migration time for propoxyphene and the resolution as a function of pH.

**Fig. 13 Variation in Migration Time and Resolution as a Function of pH**



Note that there is a correlation between the amount of time the analytes are kept on the column and the resolution; the longer the migration time, the greater the resolution. We decided to use a pH of 8.2 since at higher pH values we would begin to deprotonate propoxyphene. In addition, operating at a pH lower than the 8.2 would exceed the buffer capacity of borate. In summary, pH 8.2 gives the best combination of high resolution and a short migration time.

Table 9 shows the effect of pH on the electroosmotic and electrophoretic flow of methanol and the propoxyphene enantiomers.

**Table 9. Apparent, Electrophoretic, and Electroosmotic Mobility as a Function of pH\***

7.52	5.80E-08	5.80E-08	1.30E-08	1.20E-08	4.60E-08
8.00	5.80E-08	5.70E-08	1.20E-08	1.10E-08	4.58E-08
8.49	6.90E-08	6.80E-08	1.50E-08	1.50E-08	5.36E-08
8.98	7.30E-08	7.20E-08	9.70E-09	8.80E-09	6.32E-08
9.51	5.60E-08	5.50E-08	7.00E-09	6.20E-09	4.86E-08

\*Used 25 mM borate buffer

From this table one notes that the values for the apparent mobility,  $\mu_{app}$ , increase with increasing pH (7.52 to 8.98). However, at pH 9.51, the apparent mobility decreases for both enantiomers. The electrophoretic mobility,  $\mu_{ep}$ , on the other hand, generally decreases with increasing pH. This is consistent with the belief that increasing pH deprotonates propoxyphene, causing it to become neutral. The electroosmotic mobility,



$\mu_{eo}$ , follows the same trend as the apparent mobility. However, the  $\mu_{eo}$  decreases suddenly from pH 8.98 to pH 9.51. There is, unfortunately, no reasonable explanation for such a trend.

#### *Buffer Concentration Optimization*

We tested the effects of buffer concentration on  $\mu_{app}$ ,  $\mu_{ep}$ , and  $\mu_{eo}$ . Table 10 shows the results for this study.

**Table 10. Apparent, Electrophoretic, and Electroosmotic Mobilities for Differing Borate Buffer Concentrations**

100	7.2E-08	7.0E-08	1.1E-08	9.9E-09	6.1E-08
50	7.8E-08	7.7E-08	1.1E-08	1.0E-08	6.7E-08
25	9.0E-08	8.9E-08	1.2E-08	1.1E-08	7.8E-08
10	1.0E-07	1.0E-07	9.6E-09	8.8E-09	9.4E-08

Both the apparent and electroosmotic flow decrease with increasing buffer concentration. The decrease in  $\mu_{app}$  is directly caused by a decrease in  $\mu_{eo}$ , which, in turn, is caused by the increase in buffer concentration. The electrophoretic mobility, on the other hand, does not change significantly, and may indeed remain constant. Figure 14 is an overlay electropherogram showing the effect of buffer concentration on the mobility and resolution. Note the increase in resolution and migration time with increasing buffer concentration.

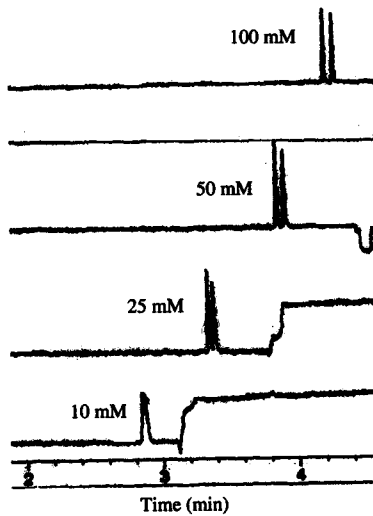


Figure 14. Electropherogram comparing results with 100 mM, 50 mM, 25 mM, and 10 mM borate buffer.

## CAPS

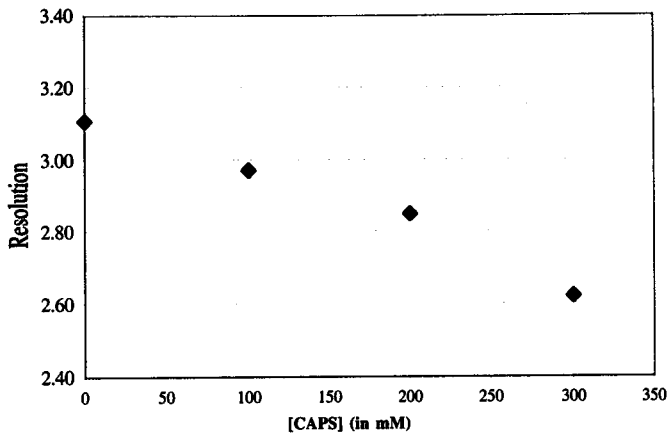
CAPS (3-[Cyclohexylamino]-1-propanesulfonic acid) is a buffer additive that prevents the adsorption of charged analytes to the capillary wall. This component was initially used since better resolution was anticipated with its use. We tested a range of CAPS concentration in the buffer including, 0 mM, 100 mM, 200 mM, and 300 mM. Table 11 lists the migration times for d- and l-propoxyphene and methanol.

**Table 11. Migration Times for l-, and d-propoxyphene and methanol**

0	4.401	4.480	5.340
100	4.652	4.732	5.682
200	4.728	4.802	5.753
300	4.878	4.948	5.962

As the concentration of CAPS increases, the migration time also increases for all three components. More compelling, however, is the change in resolution with increasing [CAPS] (Figure 15).

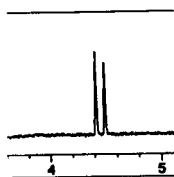
**Figure 15. Resolution vs. [CAPS]**



The resolution *decreases* with increasing [CAPS]. The best resolution is achieved when CAPS is not used.

#### *Optimal Conditions*

From these optimization studies, we determined that the optimal conditions to separate the enantiomers of propoxyphene is 30 mM heptakis tri(2,3,6-O-methyl)  $\beta$ -CD, 0 mM CAPS, pH of 8.22, and 25 mM borate buffer. Figure 16 shows an electropherogram using these conditions.



Time (min)

Figure 16. Electropherogram of l- and d-propoxyphene using 25 mM borate buffer, 30 mM heptakis tri(2,3,6-O-methyl)  $\beta$ -CD, 0 mM CAPS, and pH 8.22.

### Polymer Data

The first task we undertook was to re-test the polymers that were studied by Nerozzi and Jakubowski for propoxyphene separation. These polymers are shown in Figure 9.

The first polymer we studied was poly-L-SUGV (Table 12). We tested this using 25 mM phosphate buffer at pH 11.06. (The  $pK_a$  of the phosphate we used is 12.2.)

**Table 12. Results for poly-L-SUGV**

0.250	0.05	6.1
0.250	0.10	7.7
0.125	0.10	6.8
0.125	0.50	10.7
0.025	0.50	11.4
0.025	1.00	12.7

In all cases no separation occurred. One trend seen in Table 1 is the increase in migration time ( $t_m$ ) with increasing concentration of polymer surfactant. From these results we can deduce that there is a definite interaction between the propoxyphene and the polymer. However, this interaction does not separate the enantiomers. Also note that a lower concentration of propoxyphene produces sharper peaks. We therefore maintained a concentration of 0.025 mg/mL each of l- and d-propoxyphene in the following experiments.

Figure 17 shows some electropherograms showing the trend in migration time. The napsylate peak for each pair of data does not shift as a function of the polymer

concentration. This rules out the possibility of a viscosity effect. If a viscosity effect existed, then the napsylate peak would shift by the same amount of time. However, we do not observe this.



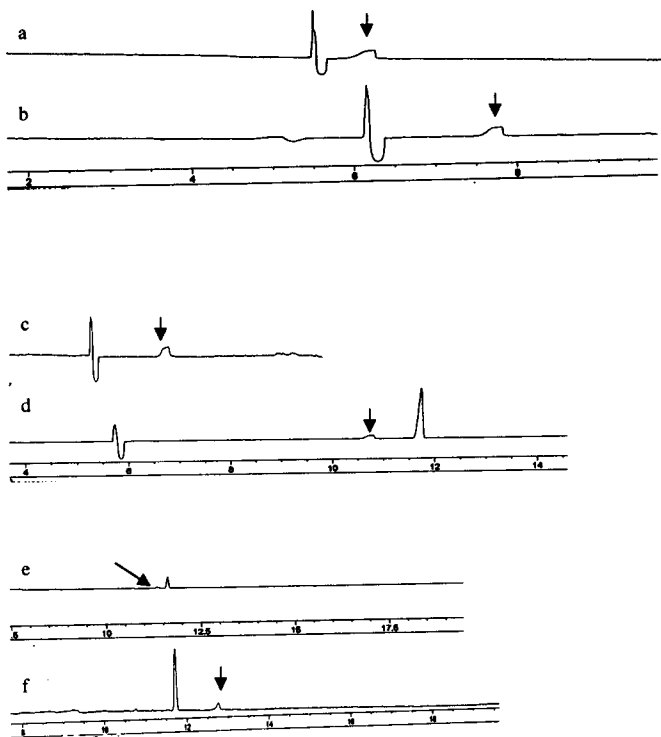


Figure 17. Electropherograms depicting: a) 0.250 mg/mL d-, l-propoxyphene with 0.05% poly-L-SUGV; b) 0.250 mg/mL d-, l-propoxyphene with 0.10% poly-L-SUGV; c) 0.125 mg/mL d-, l-propoxyphene with 0.10% poly-L-SUGV; d) 0.125 mg/mL d-, l-propoxyphene with 0.50% poly-L-SUGV; e) 0.025 mg/mL d-, l-propoxyphene with 0.50% poly-L-SUGV; and f) 0.025 mg/mL d-, l-propoxyphene with 1.00% poly-L-SUGV. The arrows show the propoxyphene signal.

We next tested poly-L-SUTBL in 25 mM borate buffer at a pH of 9.33. However, the electropherograms did not reveal any analyte peak. We suspected that the polymer was causing errors in the baseline shape. We then tried to use the same buffer at a pH of 8.20. An odd, saddle-shaped peak appeared at a migration time of six minutes. However, when we ran 1-propoxyphene alone, the same saddle appeared, indicating that the two "tips" in the saddle were not being formed by two enantiomers (Figure 18).

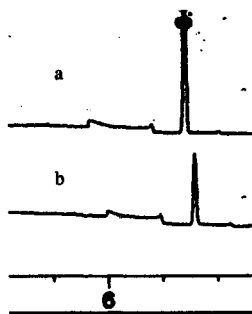


Figure 18. Electropherogram depicting: a) l- and d-propoxyphene with 0.05% poly-L-SUTBL; and b) l-propoxyphene with 0.05% poly-L-SUTBL

The next polymer we tried was poly-L-SUGA in 25 mM borate buffer at a pH of 8.17 (Table 13). We tested this polymer at a concentration of 0.05% and 0.50%. No separation occurred, but we did note once again that the  $t_m$  of the propoxyphene for each increased from 5 to 9 minutes. Therefore there is a definite interaction between the propoxyphene and the polymer. We also tried this polymer in the same concentrations using 25 mM phosphate buffer at a pH of 11.06 (Table 13). Again, there was no separation, but the  $t_m$  increased from 5.5 to 8.7 minutes with increasing polymer concentration.

**Table 13. Results for poly-L-SUGA**

0.05	25 mM Borate	8.17	5
0.50	25 mM Borate	8.17	9
0.05	25 mM Phosphate	11.06	5.5
0.50	25 mM Phosphate	11.06	8.7

The last dipeptide polymer surfactant we used was poly-L-SUVL. We tested this polymer in 25 mM phosphate buffer at a pH of 11.06 at a concentration of 0.05% and 0.50%. No separation occurred, but the  $t_m$  increased from 6 to 10.5 minutes (Table 14).

The last polymer surfactant we used was poly-L-SUV, with 25 mM borate buffer at a pH of 8.22. There was no separation of the propoxyphene peak, and the  $t_m$  of the sample was 12.3 minutes (Table 14).

**Table 14. Results for poly-L-SUVL and poly-L-SUV**

poly-L-SUVL	0.05	0.025	25 mM Phosphate	11.06	6.0
	0.50	0.025	25 mM Phosphate	11.06	10.5
poly-L-SUV	1.00	0.025	25 mM Borate	8.22	12.3
	1.00	0.100	25 mM Borate	8.22	12.0

From these polymer studies we conclude that an increase in the concentration of the polymer results in an increase of the migration time of the propoxyphene peak. This signals that there is a definite interaction between the propoxyphene and the polymers.

*Poly-L-SUThr and Derivatives*

Currently, we are examining the behaviour of the threonine polymer that we synthesized, poly-L-SUThr. We will also examine two other threonine derivatives of hexanoic acid and 4-pentenoic acid. Preliminary results with the hexanoic acid derivative of threonine do not reveal any separation of propoxyphene.

## Discussion

### *Monomer CDs*

The most compelling data from our study come from the trends seen using the heptakis di(2,6-O-methyl)  $\beta$ -CD, the dimethylated Cerestar  $\beta$ -CD, and the heptakis tri(2,3,6-O-methyl)  $\beta$ -CD (Figure 10). The degree to which the cyclodextrin is methylated increases in this order, which is also the order in which an increase in the resolution of the peaks of the enantiomers of propoxyphene is observed (Table 2). From these data it appears that the added methyl groups modify the cavity of the cyclodextrin, such that one enantiomer binds better than the other enantiomer.

In the case of the hydroxypropyl  $\beta$ -CD, it could be surmised that the longer chains fill the cavity and modify the cavity in such a way that there is no preferential binding—though this is mere speculation. Although the polymer cyclodextrins' monomer unit resembles hydroxypropyl  $\beta$ -CD in its structure, the linkers in the polymer are not able to fill the cavity since they are sterically hindered by the adjacent cyclodextrin.

We also determined that the samples could be quantified within a small range of concentrations (Figure 11). This linearity in the data allows one to construct a calibration curve and quantify data. The only drawback to the current calibration curve range is that it is quite limited; it quantifies propoxyphene concentrations ranging from 0.0125 mg/mL to 0.050 mg/mL. We were unsuccessful in our attempts to extend the upper limit of the calibration curve to 0.075 mg/mL. Nevertheless, we hypothesize that this problem arises from the software itself and not from experimental parameters. Therefore, the possibility of extending the range of quantifiable concentrations still exists.

The order of elution was determined to be 1 followed by d propoxyphene (Figure 12). This can be used by the Forensic Center in their analyses; a crime sample can be spiked with either form to determine which form is present in the sample.

The relative standard deviation for the migration time data and the integration data are within the reported error (Agilent Technologies) (Table 3). This result is crucial since this method will be used for the analysis of crime samples where reproducibility is a must.

Small, organic additives were also observed to not have a significant effect on the quality of separation of propoxyphene. Often times these additives are used to modify the cavity shape of cyclodextrins to afford better separation.<sup>20</sup> However, in the case of propoxyphene, the additives did not improve separation. The cavity of the cyclodextrin may be packed with propoxyphene such that there is not enough space for the additives to bind in the cavity.

Upon discovering that heptakis tri(2,3,6-O-methyl)  $\beta$ -CD was optimal for separating enantiomeric propoxyphene, several experiments were performed to optimize the method with respect to parameters such as buffer pH, buffer concentration, and CAPS concentration. Several interesting trends were seen with respect to these optimization experiments.

In optimizing the buffer pH, it was observed that both the resolution and migration time follow similar trends. Both have high values in the pH range of 7.5 to 8.0. At this pH range, the magnitude of the  $\zeta$  potential is large, and this in turn should increase the electroosmotic mobility (equation (2)). Indeed, from the data in Table 9, the electroosmotic mobility increases with increasing pH up to 8.98. However, above pH



8.98, the mobility decreases. Although one may surmise that propoxyphene is being deprotonated at this pH, this should not affect the electroosmotic mobility. Therefore, there is no proper explanation for this sudden decrease in the mobility. There is, moreover, a direct correlation between the migration time of the analytes and the resolution between the signals for each. This is not surprising since longer retention times of analytes often results in better separation, and hence, resolution.

By optimizing the buffer concentration, we found that increasing the concentration of the buffer not only increased the migration time of the analytes, but it also increased the resolution (Figure 14). Equation (1) indicates that an increase in the viscosity ( $\eta$ ) of the solution leads to a decrease in the mobility of the buffer. The decrease in the mobility would keep the analytes on the column longer, thus improving resolution. The concentration of buffer also directly affects the  $\zeta$  potential; an increase in the buffer concentration decreases the  $\zeta$  potential.

The last parameter that we studied in optimizing the method was the concentration of CAPS. Studies done by Nerozzi and Jakubowski indicated that adding CAPS to the background electrolyte sharpens the peak shape and improves resolution. However, in our studies, we observe that CAPS *worsens* resolution (Figure 15). Moreover, the decrease in the resolution follows a rather linear trend. There is no clear-cut explanation for these results. Indeed, one might consider that the increase in CAPS concentration would increase resolution since it effectively increases the viscosity of the buffer. However, the opposite occurs.

From our studies, we have found that a method that utilizes 30 mM heptakis tri(2,3,6-O-methyl)  $\beta$ -CD in a 25 mM borate buffer at pH 8.2 is the optimal protocol to

UN82  
M211s

MAGOON, TANIA  
CHEMISTRY

SEPARATION OF CHIRAL CONTROLLED ETC.  
HRS.

2001

2-2



separate propoxyphene. Our method has distinct advantages to the method reported by Lurie and co-workers.<sup>13</sup> Our method of separation has an analysis time of 4.5 minutes while Lurie's procedure has an analysis time of 20 minutes. We also use one CD, making this system less complex; Lurie uses two cyclodextrins in an organic solvent.

Our method also has clear advantages over the method currently used by the Forensic Center, i.e. crystallization. We obtain a hard copy of the data—data that offers much qualitative and quantitative information. Our method also requires a smaller sample; 0.025 mg/mL of propoxyphene is used in our method compared to approximately 1 mg in the Forensic Center's method.

### *Polymer Data*

We tested a variety of polymers in this section of the experiment including poly-L-SUGV (glycine-valine), poly-L-SUTBL (*tert*-butyl-leucine), poly-L-SUGA (glycine-alanine), poly-L-SUVL (valine-leucine), and poly-L-SUV (valine). In all of the cases we did not separate the enantiomers of propoxyphene. We did, however, note an increase in the migration times of the propoxyphene peak.

This increase in the migration time indicates that there is an interaction between the propoxyphene molecules and the surfactants themselves. Since no separation has occurred, we believe that the propoxyphene may be partitioning too far into the hydrophobic core of the polymer surfactant instead of interacting with the chiral center. Moreover, when these surfactants do achieve chiral separation, it may be due to the hydrogen-bonding interaction between the enantiomers and the chiral center on the surfactant. Indeed, the molecules that Warner and co-workers were able to separate with some of the aforesaid surfactants had hydrogen-bond donating capability, and the surfactants they used had hydrogen-bond accepting capability.<sup>15</sup> We manipulated this possible phenomenon in our synthesis of a polymerized chiral surfactant using threonine as the chiral center. The hydroxyl group in the amino acid is on a chiral center. We hope we can induce propoxyphene to bind at the chiral center on the surface of the polymer rather than in the micelle interior. A strong interaction between the propoxyphene at the *surface* of the polymer surfactant will increase the mass transfer rate and possibly separate the two enantiomers.

Preliminary results from this threonine polymer show some ambiguity as to what peak represents what compound. We plan to perform more experiments with this polymer to determine whether separation can be achieved. In addition, we are synthesizing other threonine-derived acids that employ hexanoic acid and 4-pentenoic acid.

### *Polymer CDs*

From the polymer CD experiments we see that additional types of cyclodextrins can be used for separating the enantiomers of propoxyphene (Table 15). We found that the best method thus far uses 30 mM of  $\gamma$ -CDP (please refer to Keiko Ota's thesis for more information). A resolution of 4.45 is achieved with this method; this resolution value is much greater than the benchmark value of 1.5, which designates baseline resolution. This method may have a slight advantage over the use of the monomer CDs since the polymers are known to be a bit more soluble than the monomers. They are more unlikely to precipitate out of solution than are the monomers. From a practical standpoint, the polymer cyclodextrins are more expensive than the monomer species; therefore, it is more economical to invest in the monomer cyclodextrin species.

## References

- (1) <http://www.usdoj.gov/dea/concern/abuse/charts/chart4/table9.htm>
- (2) <http://www.health-center.com/db/PageReq?SessionID=1366&TopicID=332&PageID=1329&Action=view>
- (3) Budavari, S (Editor). *Merck Index*, 12<sup>th</sup> ed.; Merck and Co.: New Jersey, 1996; 1347-1363.
- (4) <http://www.rxlist.com/cgi/generic3/propoxnap.htm>
- (5) Agnew-Heard, K. A., Sánchez Peña, M., Shamsi, S. A., Warner, I. M. *Anal. Chem.* **1997**, *69*, 958-964.
- (6) <http://www.scimedia.com/chem-ed/sep/electrop/cap-el.htm>
- (7) Kuhn, R., Hoffstetter-Kuhn, S. in "Chapter 2: Basic Principles," *Capillary Electrophoresis: Principles and Practice*. **1993**, Springer-Verlag, Berlin.
- (8) <http://www.ceandcec.com/cetheory.htm>
- (9) Wang, J.; Warner, I. M. *Anal. Chem.* **1994**, *66* (21), 3773-3776.
- (10) Godel, H.; Weinberger, R. Chiral Recognition by Capillary Electrophoresis with Cyclodextrins: Application Note. Hewlett Packard Manual.
- (11) Lurie, I. S. Analysis of Seized Drugs by Capillary Electrophoresis, in *Analysis of Addictive and Misused Drugs*, pp. 151-219. New York: Marcel Dekker, 1994.
- (12) <http://www.ceandcec.com/newpage12.htm>
- (13) Lurie, I. S.; Klein, R. F. X.; Dal Cason, T. A.; LeBelle, M. J.; Brenneisen, R.; Weinberger, R. E. *Anal. Chem.* **1994**, *66*, 4019-4026.

- (14) Billiot, E., Macossay, J., Thibodeaux, S., Shamsi, S. A., Warner, I. M. *Anal. Chem.* **1998**, *70*, 1375-1381.
- (15) Billiot, E., Thibodeaux, S., Shamsi, S., Warner, I. M., *Anal. Chem.* **1999**, *71*, 4044-4049.
- (16) Haddadian, F., Billiot, E. J., Shamsi, S. A., Warner, I. M. *J. Chromatography A.* **1999**, *858*, 219-227.
- (17) Billiot, E., Warner, I. M. *Anal. Chem.* **2000**, *72*, 1740-1748.
- (18) Macossay, J.; Shamsi, S.; Warner, I. M. *Tetrahedron Letters.* **1999**, *40*, 577-580.
- (19) Werner, T. C., Forrestall, K. J., McIntosh, S. L., and J. Pitha. *Applied Spectroscopy.* **2000**, *54*, 560-564.
- (20) [http://scholar.lib.vt.edu/theses/available/etd-32298-223814/unrestricted/ch\\_02.pdf](http://scholar.lib.vt.edu/theses/available/etd-32298-223814/unrestricted/ch_02.pdf)